Hydrolysis on Transition Metal Oxide Clusters and the Stabilities of M−O−M Bridges

J. R. Tobias Johnson*

Inorganic Chemistry, Department of Chemistry, Göteborg University, S-412 96 Göteborg, Sweden

Itai Panas

Department of Inorganic Environmental Chemistry, Chalmers University of Technology, S-412 96 Göteborg, Sweden

Received September 27, 1999

Water addition to molecular single, double and triple M−O−M bridges (M = Sc, Ti, V, Cr, and Mn) were considered, and the stabilities toward stepwise hydrolysis of the oxygen bridges were studied by means of quantum chemistry. The M−O bond distances for the studied systems were compared to experiment for demonstration of the applicability of the B3LYP functional to the investigated systems. While substantial exothermicities were found for the hydrolysis of double and triple M−O−M bridges, addition of water to a single bridge was generally found to be slightly endothermic. The lack of enthalpy drive for the $(OH)_yO_xM-O-MO_x(OH)_y + H_2O \rightarrow 2MO_{x-1}(OH)_{y+2}$ reaction was taken to suggest that entropy increase and the formation of mononuclear water complexe, would be decisive factors for the dissociation. A mechanism was proposed for the observed erosion of the protective chromium oxide scale on high-temperature alloys at elevated temperatures and high humidities, based on the formation of $CrO_2(OH)_2(g)$.

1. Introduction

Malleability, shine, hardness, and durability are some attractive properties of metals. However, a pure metal may not prove optimal for any such property, and the earliest improvement focused in particular on obtaining a harder material. Thus, ancient metallurgy solved the problem of copper axes being too soft for everyday use by alloying the copper with tin, producing bronze. Apart from the mechanical properties, durability in a corrosive atmosphere and cost efficiency are other necessary prerequisites. The continued search for improved materials led to an evolutionary development of metallurgy, which is reflected in our everyday utensils. The functionality of particular steels is adjusted in detail by alloying iron with metals such as chromium, vanadium, nickel, and manganese. We understand today that the ability of steels to withstand corrosion depends critically on the chemical and mechanical stabilities of its surface oxides. While some elements are added for improving the mechanical properties, others are added mainly to protect iron from destructive oxidation. Particularly, chromium-rich alloys are known for being protected by very stable surface oxides.

Exposure to a humid atmosphere at elevated temperatures comprises one sensitive chemical parameter for investigating the stability of an alloy.[1,2] Such a treatment of chromium-rich steels reportedly results in a dramatically increased weathering of the thin protective chromium oxide scale, as molecular chromium oxyhydroxides are emitted and observed to condense as chromium oxide downstream in the reaction chamber.[2] In this context, the objective of two previous studies was to investigate the affinity of the metal−oxygen chemical bond toward water addition.[3,4] In order to distinguish between general and specific properties for a particular metal, Ge was chosen to represent the p-elements,[3] while the Sc−Mn sequence was used for the d-elements.[4] Three classes of chemical bonds are found for the Sc−Mn sequence, comprising single M−O bonds of local σ symmetry, multiple M═O bonds, involving one or two M $3d_\pi$ to O $2p_\pi$ components and M···OH_x complex bonds, used in water complexes and hydroxide bridges. These types of bonds are commonly found in transition metal oxide solids. Hence, an essential semiquantitative test for the results obtained in the present study, as well as in ref 4, comprises comparing calculated bond lengths with those determined by means of crystallography.

While the previous investigation addressed the stabilities of mononuclear oxides and oxyhydroxides toward water addition,[4] the present study focuses on the water chemistry of binuclear transition metal oxide clusters. A systematic study on the reactivities of oxide clusters containing single, double, and triple M−O−M bridges toward successive water additions, i.e. reactions that produce an increasing number of hydroxide groups, is performed. The calculated relative stabilities of the various oxides, oxyhydroxides, and hydroxides are proposed to be useful as indicators on the chemical stability of similar surface oxides. Following this claim, the possible relevance to various aspects of chromium oxide surface erosion is discussed.

(1) Ebbinghaus, B. B. *Combust. Flame* **1995**, *101*, 311.
(2) Asteman, H.; Svensson, J.-E.; Johansson, L.-G.; Norell, M. *Oxid. Met.* **1999**, *52*, 161.
(3) Johnson, J. R. T.; Panas, I. *Chem. Phys.* **1999**, *249*, 273.
(4) Johnson, J. R. T.; Panas, I. *Inorg. Chem.* **2000**, 39, xxxxx.

10.1021/ic991144l CCC: $19.00
Published on Web 06/27/2000

Results are presented for the reactions

$$Sc_2O_3(g) + 5H_2O(g) \rightarrow 2Sc(OH)_3{\cdot}H_2O(g) \quad (R1)$$

$$Ti_2O_4(g) + 4H_2O(g) \rightarrow 2Ti(OH)_4(g) \quad (R2)$$

$$V_2O_5(g) + 3H_2O(g) \rightarrow 2VO(OH)_3(g) \quad (R3)$$

$$Cr_2O_6(g) + 2H_2O(g) \rightarrow 2CrO_2(OH)_2(g)$$
$$Cr_2O_6(g) + 4HF(g) \rightarrow 2CrF_2O_2(g) + 2H_2O(g) \quad (R4)$$

$$Mn_2O_7(g) + H_2O(g) \rightarrow 2MnO_3(OH)(g) \quad (R5)$$

The parallel investigation in R4 on the reactivity of molecular Cr_2O_6 with fluoric acid (HF(g)) is yet another test for internal consistency, taking F to be an OH analogue. In this context, it is interesting to note that a marked acceleration in the deterioration of the protecting oxide scale has been observed when steel was exposed to moist air in the presence of HCl(g).[5]

2. Methods

We understand today the interactions of electrons and nuclei in a molecule. Density functional theory (DFT) comprises one efficient realization of this understanding, provided that ground-state properties of any particular molecular system are sought. The basis for DFT is the Hohenberg−Kohn theorem, which states that the ground-state electron density is sufficient for representing all *ground-state* properties of a many-electron system.[6] It is the exploration of this limitation which makes it so efficient for chemical purposes. While the existence of a universal functional has been proven, no unique prescription for how to systematically improve on any such approximation exists. This implies that practical DFT formulations are semiempirical and must be used with caution. Still, considerable robustness of DFT is expected, because in producing the required one-particle density matrix the Kohn−Sham orbitals are employed.[7] These differ only slightly from the orbitals produced in Hartree−Fock (HF) theory. DFT deviates qualitatively from HF when it comes to *how* the one-particle density is employed to produce the effective single-particle Hamiltonian, analogous to the Fock operator. Thus HF exchange interaction is replaced by an exchange-correlation functional in DFT. This modification does the work which normally requires the significantly more time-consuming explicit electron correlation treatments of ab initio quantum chemistry.

There are presently several exchange-correlation potentials to choose from. The B3LYP hybrid functional[8] is employed in the present study after careful investigations and benchmark calculations using ab initio quantum chemistry on several ScO_x molecules and ions.[9,10] These systems display the main features of transition metal−oxygen chemical bonding. The ScO_2 molecule is in fact one of the most complex transition metal dioxide systems, because of its flexible electronic structure. In order to test B3LYP on chemically more relevant problems, several other Sc_xO_y species were also systematically investigated, for which results were compared to experimental findings.[11] An internally consistent understanding of bonding and stabilities for these systems emerged, which also were in agreement with experimental results.

3. Computational Details

Calculations using DFT with the B3LYP functional were performed on the transition metal oxides, oxyfluorides, and oxyhydroxides involved in the intermediary reaction steps of R1−R5 and on water. Molecular structures were optimized and analytical Hessians evaluated, producing energies and vibrational spectra by employing the GAUSSIAN program package.[12] The 6-311G(d) basis set was used for Sc, Ti, V, Cr, and Mn together with the small 6-311G basis sets (denoted by (S)) for O, F, and H atoms. The larger 6-311+G(2df,2pd) basis sets (L) were used for the first reaction steps, in order to get higher accuracy and thus check the applicability of (S). All calculations were carried out on closed shell singlet systems, i.e. the ground states of the investigated species in their highest oxidation state.

4. Results and Discussion

Systematic investigations are presented for the stepwise addition of molecular water to transition metal oxide clusters, which contain M−O−M bridges, thus increasing the number of M−OH units by two in each addition step. The study addresses hydrolysis on binuclear oxide clusters of Sc, Ti, V, Cr, and Mn with homogeneous metal composition. Regarding the single-bridge systems, the terminal OH groups can be understood to truncate an envisaged polymeric structure. Such polymers are in particular known to exist for vanadium and chromium. Thus the metavanadates contain $[-O-(VO_2)-O-(VO_2)-]$ chains of formal $(VO_3)_n^{n-}$ composition with alkali counterions. These chains are thus isoelectronic analogues to $CrO_3(s)$, which is known to consist of $[-O-(CrO_2)-O-(CrO_2)-]$ chain polymers.[13] While Mn does not form $[-(MO_x)-O-(MO_x)-]$ infinite chains, bridging and nonbridging oxygens are observed in the molecular crystal of $Mn_2O_7(s)$, the so-called permanganic acid anhydride.[13,14] Hence, the molecular Mn system comprises a real illustration for addition of water to an M−O−M bridge. Structures of molecular ions containing Sc_xO_y and Ti_xO_y put the findings for vanadium, chromium, and manganese into a broader context. The oxides of Ti contrast the chromates and metavanadates, since in the titanates the $(TiO_3)_n^{2n-}$ ions produce the three-dimensional perovskite cage structure, with has the metal in an octahedral position rather than tetrahedrally coordinated, as in the chain polymers.[14] It may be interesting to note in this context that these cage structures reappear when moving down in the V (Nb, Ta) and Cr (Mo, W) groups, e.g. in $KTaO_3$ and WO_3, respectively.

Water addition to mononuclear transition metal oxides and oxyhydroxides has been investigated for the same metal sequence (Sc−Mn) as in the present work.[4] The main result was that water addition to the mononuclear systems is exothermic when the metal ion has less than tetrahedral configuration.

(5) Asteman, H.; Svensson, J.-E.; Johansson, L.-G.; Norell, M. Work in progress.
(6) Hohenberg, P.; Kohn, W. *Phys. Rev. B* **1964**, *136*, 864.
(7) Kohn W.; Sham, L. J. *Phys. Rev. A* **1965**, *140*, 1133.
(8) Becke, A. D. *J. Chem. Phys.* **1993**, *98*, 5648.
(9) Bauschlicher, C. W.; Zhou, M.; Andrews, L.; Johnson, J. R. T.; Panas, I.; Snis, A.; Roos, B. O. *J. Chem. Phys. A* **1999**, *103*, 5463.
(10) Johnson, J. R. T.; Snis, A.; Panas, I.; Roos, B. O. In preparation.
(11) Johnson, J. R. T.; Panas, I. *Chem. Phys.* **1999**, *248*, 161.
(12) Frisch, M. J.; Trucks, G. W.; Schlegel, H. B.; Gill, P. M. W.; Johnson, B. G.; Robb, M. A.; Cheeseman, J. R.; Keith, T.; Petersson, G. A.; Montgomery, J. A.; Raghavachari, K.; Al-Laham, M. A.; Zakrzewski, V. G.; Ortiz, J. V.; Foresman, J. B.; Peng, C. Y.; Ayala, P. Y.; Chen, W.; Wong, M. W.; Andres, J. L.; Replogle, E. S.; Gomperts, R.; Martin, R. L.; Fox, D. J.; Binkley, J. S.; Defrees, D. J.; Baker, J.; Stewart, J. P.; Head-Gordon, M.; Gonzalez, C.; Pople, J. A. *Gaussian 94,* revision B.3; Gaussian, Inc.: Pittsburgh, PA, 1995.
(13) Greenwood, N. N.; Earnshaw, A. *Chemistry of the Elements*, 2nd ed.; Butterworth-Heinemann: Oxford, 1997.
(14) Wells, A. F. *Structural Inorganic Chemistry*, 5th ed.; Oxford University Press: Oxford, 1984.

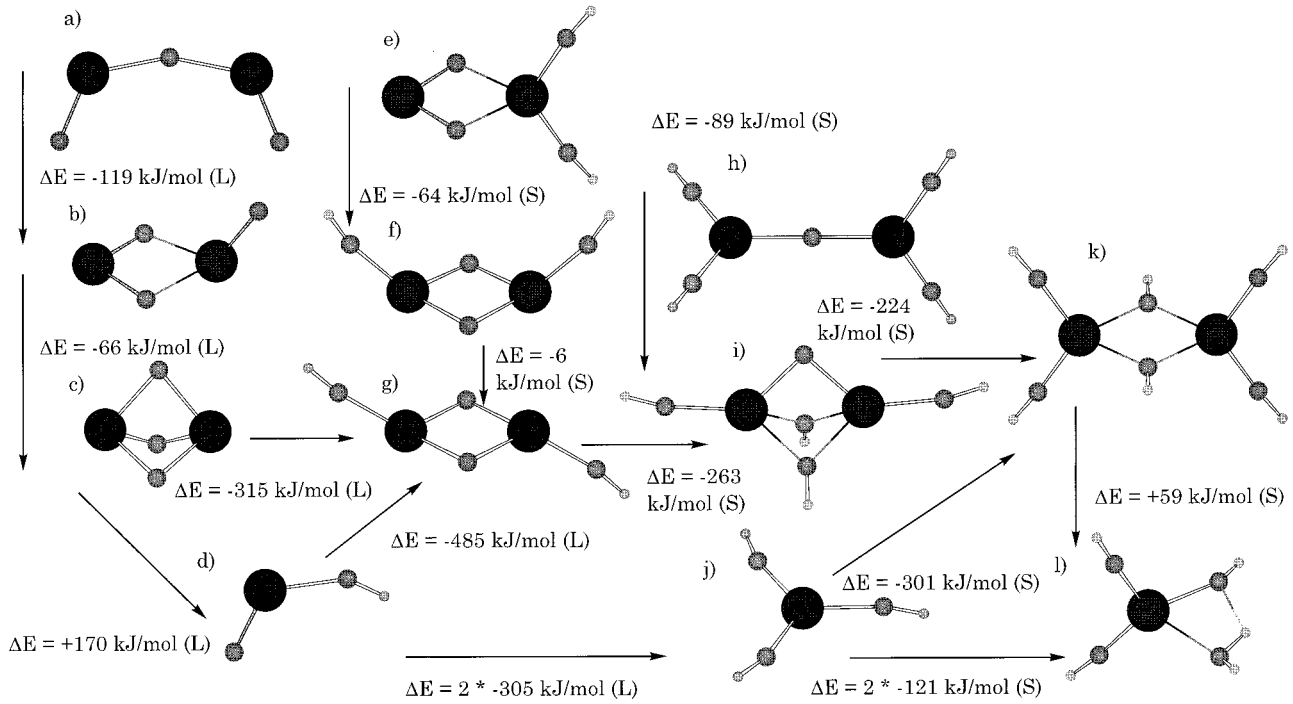

Figure 1. Structures in the $Sc_2O_3 + 5H_2O$ system together with relative stabilities and energetics for some hydrolysis reactions. Sc_2O_3: (a) $OScOScO$ (C_{2v}), (b) ScO_2ScO (C_s), (c) ScO_3Sc (D_{3h}). $Sc_2O_4H_2$: (d) $2(ScO)OH$ (C_s), (e) $ScO_2Sc(OH)_2$ (C_{2v}), (f) $HOScO_2ScOH$ (C_{2v}), (g) $HOScO_2ScOH$ (C_{2h}). $Sc_2O_5H_4$: (h) $(HO)_2ScOSc(OH)_2$ (D_{2d}), (i) $HOScO(OH)_2ScOH$ (C_{2v}). $Sc_2O_6H_6$: (j) $2Sc(OH)_3$ (C_{3h}), (k) $(HO)_2Sc(OH)_2Sc(OH)_2$ (D_{2h}), (l) $2Sc(OH)_3 \cdot H_2O$ (C_1).

Additional water molecules will produce hydrogen-bonded complexes and finally solvate the metal species. Similar results were obtained for the germanium oxyhydroxides, in the case of which both mono- and polynuclear oxides were studied.[3] Below, the results for Ge are compared with those obtained for the isoelectronic Ti systems.

Rather than addressing the actual process of metal oxidation, this study concerns the stability of transition metal oxides to water-induced deterioration. The computational procedure implies full geometry optimization of each system, i.e. all reactants and products. This is complemented by a vibrational analysis, in order to find model structures that are local energy minima. For several of the model species, there exist more than one minimum structure within the same stoichiometry. It becomes important for the chemical understanding to characterize structures and paths as well as energy minima, and to evaluate relative stabilities along the reaction coordinates. Summaries of geometrical parameters, vibrational frequencies, and corresponding IR intensities for these structures are provided in Tables 1−6 and illustrated in Figures 1−6. The M−O bond distances found for the model systems are compared to crystallographic data in Figure 7 in order to substantiate the applicability of the B3LYP approach.

4.1. $Sc_2O_3 + 5H_2O$. One natural starting point for modeling water addition to binuclear scandium oxides in general and an Sc−O−Sc bridge in particular becomes the Sc_2O_3(g) system, which has been investigated previously.[11] The bent O═Sc−O−Sc═O chain (Figure 1a) is floppy, with a transition state (TS) in the planar structure of C_{2v} symmetry. Rotation of the O═Sc units out of the molecular plane into a C_2 structure releases some 10−20 kJ/mol. The same energy scale is observed for dissociative water addition to the oxygen bridge in the TS structure, as the production of two O═Sc−OH(g) molecules (Figure 1d) is exothermic by 15 kJ/mol (L). Such marginal reactivity is one general property of the single-bridged M−O−M systems studied in the present work.

The O═Sc−O−Sc═O chain structure is not stable, but collapses to a trigonal bipyramid Sc{O_3}Sc cluster (Figure 1c) with D_{3h} symmetry, and is thus stabilized by 185 kJ/mol (L).[11] Alternatively, a stable $ScO_2\cdots ScO^+$ complex (Figure 1b) can be formed. The two units are connected through two complex Sc···O bonds (2.12 Å) in a distorted ScO_2Sc ring. While being 119 kJ/mol (L) more stable than the chain structure, the complex is still 66 kJ/mol (L) above the ScO_3Sc cluster.[11] Water addition to the complex produces $Sc<O_2>Sc<(OH)_2$ (Figure 1e), which models water addition to an Sc═O bond rather than to an oxygen bridge. This $ScO_2\cdots Sc(OH)_2^+$ complex still displays two long Sc···O bonds (2.08 Å) in the central ring, originating from the anhydrate.

A more suitable model than the chain or complex structures for water addition to scandium oxides may be the reaction with one of the three equivalent Sc−O−Sc bridges in ScO_3Sc(g). This addition reaction produces $HO-Sc<O_2>Sc-OH$(g), which has a structure based on a symmetric ScO_2Sc ring. Such rings were found to be important building blocks in molecular scandium oxides.[11] There are two stable conformations for this system, i.e. with the OH groups cis (Figure 1f) and trans (Figure 1g), respectively. The latter structure is 6 kJ/mol (S) more stable than the former, which in turn is 64 kJ/mol (S) below the ScO_2-$Sc(OH)_2$ complex. Similar to $(HO)ScO_2Sc(OH)$, the triplet $OScO_2ScO$ system displayed potential energy minima for both cis and trans structures.[6] Characteristic for both structures are (a) the similar Sc−O bond distances, 1.91 Å (S and L) within the ring and 1.88 Å (S) and 1.90 Å (L) to the terminal OH groups, and (b) the 166°(S)−168°(L) Sc−O−H bond angles.

Water addition to ScO_3Sc(g), forming the C_{2h} structure, is exothermic by 343 kJ/mol (S) and 315 kJ/mol (L). This is in contrast to the minor exothermicity obtained above for the single-bridged system and illustrates the degree to which the Sc−O−Sc bridges in the trigonal bipyramid cluster are strained. The joining of two ScO(OH) molecules into an $(HO)ScO_2Sc$-

Table 1. Summaries of Bond Lengths R (Å) and Bond Angles A (deg), and Ranges of Vibrational Frequencies (cm^{-1}), Together with Normal Mode Symmetries and the Number of Vibrations in Each Group, for the Sc Systems

		OScOScO	
C_{2v}	R(Sc═O): 1.695	A(Sc−O−Sc): 158.0	
(L)	R(Sc−O): 1.941	A(O═Sc−O): 123.9	
	A_2 (1 vib): 64*i*	$A_1 + B_1 + B_2$ (3+1+2 vib): 63−778	
	$A_1 + B_2$ (1+1 vib): 941−960		
		ScO_2ScO	
C_s	R(Sc═O): 1.707−1.788	A(O═Sc═O): 94.2	A(Sc═O···Sc): 94.4−119.6
(L)	R(Sc···O): 2.120	A(O···Sc···O): 76.3	
	$A' + A''$ (3+2 vib): 81−362	$A' + A''$ (1+1 vib): 506−739	
	A' (2 vib): 860−926		
		ScO_3Sc	
D_{3h}	R(Sc−O): 1.922	A(O−Sc−O): 83.4	A(Sc−O−Sc): 79.6
(S)	$A_1' + E' + E''$ (1+1+1 vib): 257−503	$A_1' + A_2'' + E'$ (1+1+1 vib): 649−744	
D_{3h}	R(Sc−O): 1.923	A(O−Sc−O): 83.5	A(Sc−O−Sc): 79.5
(L)	$A_1' + E' + E''$ (1+1+1 vib): 273−497	$A_1' + A_2'' + E'$ (1+1+1 vib): 644−744	
		$ScO_2Sc(OH)_2$	
C_{2v}	R(Sc−O): 1.782−1.878	A(Sc−O−H): 172.8	A(Sc−O···Sc): 95.1
(S)	R(Sc···O): 2.079	A(O···Sc···O): 76.8	A(O−Sc−O): 92.9−121.3
	R(O−H): 0.959		A(O−Sc···O): 112.6
	$A_1 + A_2 + B_1 + B_2$ (6+2+4+4 vib): 67−868	$A_1 + B_2$ (1+1 vib): 3886	
		$(HO)ScO_2Sc(OH)$	
C_{2v}	R(Sc−O): 1.877−1.909	A(Sc−O−H): 166.1	A(Sc−O−Sc): 95.2
(S)	R(O−H): 0.960		A(O−Sc−O): 84.6−123.6
	$A_1 + A_2 + B_1 + B_2$ (6+3+3+4 vib): 63−752	$A_1 + B_2$ (1+1 vib): 3875	
C_{2h}	R(Sc−O): 1.876−1.907	A(Sc−O−H): 167.8	A(Sc−O−Sc): 95.3
(S)	R(O−H): 0.959		A(O−Sc−O): 84.7−121.8
	$A_g + A_u + B_g + B_u$ (5+3+3+5 vib): 65−752	$A_g + B_u$ (1+1 vib): 3878	
C_{2h}	R(Sc−O): 1.905−1.913	A(Sc−O−H): 168.0	A(Sc−O−Sc): 95.3
(L)	R(O−H): 0.953		A(O−Sc−O): 84.7−127.6
	$A_g + A_u + B_g + B_u$ (5+3+3+5 vib): 41−719	$A_g + B_u$ (1+1 vib): 3972−3973	
		$(HO)_2ScOSc(OH)_2$	
D_{2d}	R(Sc−O): 1.872−1.883	A(Sc−O−H): 179.0	A(Sc−O−Sc): 180.0
(S)	R(O−H): 0.959		A(O−Sc−O): 118.0−123.9
	B_1 (1 vib): 18*i*	$A_1 + A_2 + B_1 + B_2 + E$ (4+1+1+5+6 vib): 22−882	
		$A_1 + B_2 + E$ (1+1+1 vib): 3886−3887	
D_{2d}	R(Sc−O): 1.888−1.897	A(Sc−O−H): 175.3	A(Sc−O−Sc): 180.0
(L)	R(O−H): 0.953		A(O−Sc−O): 118.5−123.0
B_1 (1 vib): 22*i*			
$A_1 + B_2 + E$ (1+1+1 vib): 3976−3977		$A_1 + A_2 + B_1 + B_2 + E$ (4+1+1+5+6 vib): 27−844	
		$(HO)ScO(OH)_2Sc(OH)$	
C_{2v}	R(Sc−O): 1.877−1.899	A(Sc−O−H): 167.2	A(Sc−O−Sc): 90.6
(S)	R(Sc···O): 2.111	A(Sc···O−H): 138.6	A(Sc···O···Sc): 79.5
	R(O−H): 0.960−0.962	A(O···Sc···O): 78.9	A(O−Sc−O): 131.2
			A(O−Sc···O): 81.4−132.0
		$A_1 + A_2 + B_1 + B_2$ (8+4+5+6 vib): 60−777	
		$A_1 + B_1 + B_2$ (2+1+1 vib): 3837−3873	
		$(HO)_2Sc(OH)_2Sc(OH)_2$	
D_{2h}	R(Sc−O): 1.860	A(Sc−O−H): 175.0	A(Sc···O···Sc): 100.5
(S)	R(Sc···O): 2.080	A(Sc···O−H): 129.7	A(O−Sc−O): 116.9
	R(O−H): 0.959−0.964	A(O···Sc···O): 79.5	A(O−Sc···O): 113.7
		$A_{g/u} + B_{1g/u} + B_{2g/u} + B_{3g/u}$ (7+6+7+7 vib): 20−774	
		$A_g + B_{1g/u} + B_{3u}$ (2+2+1 vib): 3827−3892	
		ScO(OH)	
C_s	R(Sc═O): 1.688	R(O−H): 0.958	A(O═Sc−O): 123.4
(L)	R(Sc−O): 1.926		A(Sc−O−H): 145.5
	$A' + A''$ (4+1 vib): 173−958	A' (1 vib): 3935	
		$Sc(OH)_3$	
C_{3h}	R(Sc−O): 1.864	A(O−Sc−O): 120.0	
(S)	R(O−H): 0.959	A(Sc−O−H): 179.0	
	$A' + A'' + E' + E''$ (2+2+3+1 vib): 84−773	$A' + E'$ (1+1 vib): 3889	
C_{3h}	R(Sc−O): 1.884	A(O−Sc−O): 120.0	
(L)	R(O−H): 0.954	A(Sc−O−H): 163.5	
	$A' + A'' + E' + E''$ (2+2+3+1 vib): 91−725	$A' + E'$ (1+1 vib): 3968−3970	
		$Sc(OH)_3 \cdot H_2O$	
C_1	R(Sc−O): 1.864−1.959	A(Sc−O−H): 151.7−174.8	A(O−Sc−O): 117.1−117.3
(S)	R(Sc···O): 2.192	A(Sc−O···H): 77.6	A(O−Sc···O): 73.2−115.9
	R(O−H): 0.959−0.997	A(Sc···O−H): 86.8−143.0	A(O−H···O): 122.4
	R(O···H): 1.800	A(H−O−H): 117.3	
	A (18 vib): 69−837	A (2 vib): 1549−3248	
	A (3 vib): 3865−3890		

(OH) cluster becomes exothermic by 485 kJ/mol (L), which is similar to what was previously observed for two Sc═O bonds toward forming an ScO_2Sc ring.[11] Similar basis set effects on the reactivities, i.e. ∼30 kJ/mol lowering when using (L) instead of (S), were obtained for the different additive routes. It is possible to join several ScO_2Sc rings by Sc−O−Sc bridges,

Table 2. Summaries of Bond Lengths R (Å) and Bond Angles A (deg), and Ranges of Vibrational Frequencies (cm^{-1}), Together with Normal Mode Symmetries and the Number of Vibrations in Each Group, for the Ti Systems

$OTiO_2TiO$

D_{2h} R(Ti═O): 1.631 A(O═Ti−O): 136.3 A(Ti−O−Ti): 92.5
(L) R(Ti−O): 1.882 A(O−Ti−O): 87.5
$B_{2g} + B_{3u}$ (1+1 vib): 224i−187i
$A_g + B_{1u} + B_{2u} + B_{3g/u}$ (3+2+2+4 vib): 99−1060

C_{2v} R(Ti═O): 1.616 A(O═Ti−O): 120.7 A(Ti−O−Ti): 94.8
(S) R(Ti−O): 1.851 A(O−Ti−O): 85.0
$A_1 + A_2 + B_1 + B_2$ (4+2+2+2 vib): 106−740
$A_1 + B_2$ (1+1 vib): 1046−1078

C_{2h} R(Ti═O): 1.618 A(O═Ti−O): 121.3 A(Ti−O−Ti): 94.9
(S) R(Ti−O): 1.845 A(O−Ti−O): 85.1
$A_g + A_u + B_g + B_u$ (3+2+2+3 vib): 96−746
$A_g + B_u$ (1+1 vib): 1051−1067

C_{2h} R(Ti−O): 1.849 A(O═Ti−O): 124.2 A(Ti−O−Ti): 94.7
(L) R(Ti═O): 1.623 A(O−Ti−O): 85.3
$A_g + A_u + B_g + B_u$ (3+2+2+3 vib): 96−731
$A_g + B_u$ (1+1 vib): 1030−1050

(HO)OTiOTiO(OH)

C_2 R(Ti═O): 1.617 A(Ti−O−H): 151.1 A(Ti−O−Ti): 178.6
(S) R(Ti−O): 1.807−1.823 A(O−Ti−O): 120.0 A(O═Ti−O): 112.4−115.9
R(O−H): 0.961
A + B (9+7 vib): 36−938
A + B (1+1 vib): 1063−1069
A + B (1+1 vib): 3859−3860

$OTiO(OH)_2TiO$

C_{2v} R(Ti═O): 1.611 A(Ti−O−H): 141.2 A(Ti−O−Ti): 85.6
(S) R(Ti−O): 1.856 A(O−Ti···O): 84.3 A(Ti···O···Ti): 76.4
R(Ti···O): 2.038 A(O···Ti···O): 81.5 A(O═Ti−O): 120.4
R(O−H): 0.962 A(O═Ti···O): 134.2
$A_1 + A_2 + B_1 + B_2$ (6+3+4+4 vib): 102−797
$A_1 + B_2$ (1+1 vib): 1070−1105
$A_1 + B_1$ (1+1 vib): 3854−3856

$(HO)TiO_2TiO(OH)$

C_s R(Ti═O): 1.615 A(Ti−O−H): 146.1−159.1 A(Ti−O−Ti): 95.4
(S) R(Ti−O): 1.718−1.812 A(O−Ti−O): 93.1−117.5 A(O═Ti−O): 115.9
R(Ti···O): 2.024 A(O−Ti···O): 116.7 A(O═Ti···O): 112.6
R(O−H): 0.960−0.962 A(O···Ti···O): 76.1
A′ + A″ (9+8 vib): 63−827
A′ (2 vib): 919−1071
A′ (2 vib): 3843−3882

$(HO)TiO_3Ti(OH)$

D_{3h} R(Ti−O): 1.792−1.859 A(Ti−O−H): 180.0 A(Ti−O−Ti): 80.5
(S) R(O−H): 0.959 A(O−Ti−O): 82.8−130.3
$A_1' + A_2'' + E' + E''$ (2+2+4+3 vib): 27−891
$A_1' + A_2''$ (1+1 vib): 3898−3900

$OTiO_2Ti(OH)_2$

C_s R(Ti−O): 1.778−1.846 A(Ti−O−H): 163.8−168.3 A(Ti−O−Ti): 95.4
(S) R(Ti═O): 1.616 A(O−Ti−O): 84.3−116.4 A(O═Ti−O): 113.0
R(O−H): 0.958−0.959
A′ + A″ (10+7 vib): 79−803
A′ (2 vib): 858−1066
A′ (2 vib): 3905−3913

$(HO)OTiOTi(OH)_3$

C_1 R(Ti−O): 1.777−1.821 A(Ti−O−H): 150.4−173.4 A(Ti−O−Ti): 167.4
(S) R(Ti═O): 1.617 A(O−Ti−O): 107.8−120.3 A(O═Ti−O): 114.1−115.5
R(O−H): 0.957−0.961
A (24 vib): 19−835
A (2 vib): 930−1067
A (4 vib): 3858−3926

$(HO)OTi(OH)_2TiO(OH)$

C_{2h} R(Ti═O): 1.612 A(Ti−O−H): 145.6 A(Ti···O···Ti): 99.4
(S) R(Ti−O): 1.801 A(Ti···O−H): 130.3 A(O═Ti−O): 112.1
R(Ti···O): 2.012 A(O−Ti···O): 116.5 A(O═Ti···O): 113.9
R(O−H): 0.963 A(O···Ti···O): 80.6
$A_g + A_u + B_g + B_u$ (8+4+6+9 vib): 28−1081
$A_g + A_u + B_u$ (2+1+1 vib): 3835−3839

C_{2v} R(Ti═O): 1.612 A(Ti−O−H): 148.1 A(Ti···O···Ti): 98.1
(S) R(Ti−O): 1.800 A(Ti···O−H): 127.3 A(O═Ti−O): 113.0
R(Ti···O): 2.011 A(O−Ti···O): 116.8 A(O═Ti···O): 112.6
R(O−H): 0.961−0.965 A(O···Ti···O): 81.3
$A_1 + A_2 + B_1 + B_2$ (9+5+5+7 vib): 60−1087
$A_1 + B_1 + B_2$ (2+1+1 vib): 3816−3850

$(HO)_2TiO_2Ti(OH)_2$

D_{2h} R(Ti−O): 1.777−1.832 A(Ti−O−H): 175.6 A(Ti−O−Ti): 95.8
(S) R(O−H): 0.957 A(O−Ti−O): 84.2−116.0
$A_{g/u} + B_{1g/u} + B_{2g/u} + B_{3g/u}$ (7+6+7+6 vib): 71−874
$A_g + B_{1g} + B_{2u} + B_{3u}$ (1+1+1+1 vib): 3919−3923

$(HO)_3TiOTi(OH)_3$

C_2 R(Ti−O): 1.777−1.834 A(Ti−O−H): 129.4−164.4 A(Ti−O−Ti): 119.6
(S) R(O−H): 0.959−0.979 A(Ti···O−H): 100.8 A(O−Ti−O): 99.7−114.1
R(O···H): 2.024 A(H−O···H): 116.3 A(O−H···O): 138.8
A + B (16+16 vib): 43−887
A + B (1+1 vib): 3554−3563
A + B (2+2 vib): 3837−3905

D_3 R(Ti−O): 1.779−1.803 A(Ti−O−H): 180.0 A(Ti−O−Ti): 180.0
(S) R(O−H): 0.957 A(O−Ti−O): 108.4−110.5
$A_1 + A_2 + E$ (6+5+11 vib): 22−936
$A_1 + A_2 + E$ (1+1+2 vib): 3928−3933

TiO_2

$C_{\infty v}$ R(Ti═O): 1.634 A(O═Ti═O): 111.5
(S) A_1 (1 vib): 377 $A_1 + B2$ (1+1 vib): 1013−1040
$C_{\infty v}$ R(Ti═O): 1.638 A(O═Ti═O): 112.1
(L) A_1 (1 vib): 348 $A_1 + B2$ (1+1 vib): 990−1035

$TiO(OH)_2$

C_s R(Ti═O): 1.614 R(O−H): 0.961 A(O═Ti−O): 115.3
(S) R(Ti−O): 1.809 A(Ti−O−H): 151.7 A(O−Ti−O): 121.1
A′ + A″ (6+4 vib): 101−1073
A′ + A″ (1+1 vib): 3861−3864

C_s R(Ti═O): 1.615 R(O−H): 0.959 A(O═Ti−O): 117.4
(L) R(Ti−O): 1.835 A(Ti−O−H): 133.5 A(O−Ti−O): 121.3
A′ + A″ (6+4 vib): 79−1065
A′ + A″ (1+1 vib): 3897−3900

$Ti(OH)_4$

C_1 R(Ti−O): 1.779 A(O−Ti−O): 109.4−109.5
(S) R(O−H): 0.957 A(Ti−O−H): 172.3−177.6
A (18 vib): 26−831
A (4 vib): 3925−3932

formed in the condensation reaction of two Sc−OH units, into a $(ScO_2ScO)_n$ polymer structure. Close packing of such polymers and formation of octahedrally coordinated Sc atoms is favorable, as observed in Sc_2O_3(s).

Addition of a second water molecule to the double-bridged $(HO)ScO_2Sc(OH)$ cluster opens up the central ScO_2Sc ring, as the single-bridged $(HO)_2>Sc-O-Sc<(OH)_2$ molecule (Figure 1h) is formed. This oxygen bridge is found to be linear, and the Sc−O−H bond angles are nearly linear (179° (S) and 175° (L)), which suggest that electrostatic interactions dominate this

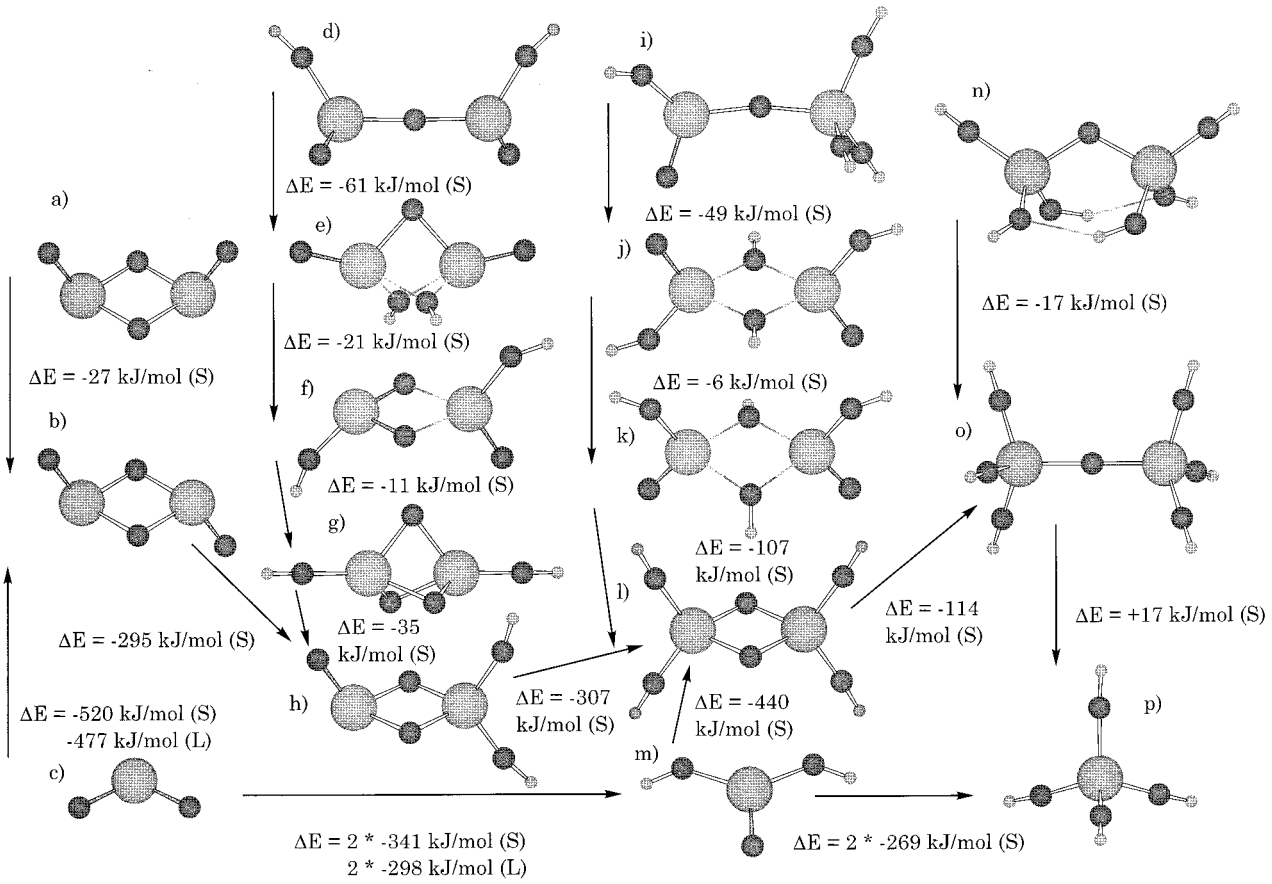

Figure 2. Structures in the $Ti_2O_4 + 4H_2O$ system together with relative stabilities and energetics for some hydrolysis reactions. Ti_2O_4: (a) $OTiO_2TiO$ (C_{2v}), (b) $OTiO_2TiO$ (C_{2h}), (c) $2TiO_2$ (C_{2v}). $Ti_2O_5H_2$: (d) HO(TiO)O(TiO)OH (C_2), (e) $OTiO(OH)_2TiO$ (C_{2v}), (f) $HOTiO_2(TiO)OH$ (C_s), (g) $HOTiO_3TiOH$ (D_{3h}), (h) $OTiO_2Ti(OH)_2$ (C_s). $Ti_2O_6H_4$: (i) $HO(TiO)OTi(OH)_3$ (C_1), (j) $(HO)OTi(OH)_2TiO(OH)$ (C_{2h}), (k) $(HO)OTi(OH)_2TiO(OH)$ (C_{2v}), (l) $(HO)_2TiO_2Ti(OH)_2$ (D_{2h}), (m) $2TiO(OH)_2$ (C_s). $Ti_2O_7H_6$: (n) $(HO)_3TiOTi(OH)_3$ (C_2), (o) $(HO)_3TiOTi(OH)_3$ (D_3), (p) $2Ti(OH)_4$ (C_1).

system. However, both the planar D_{2h} and the somewhat more stable staggered D_{2d} structure displayed small symmetry-breaking vibrations. The addition reaction leading to the latter structure is exothermic by 174 kJ/mol (S) and 141 kJ/mol (L). A continued search for the minimum energy structure results in a significant bending of the linear Sc−O−Sc bridge followed by the formation of two Sc···(OH)···Sc bridges. The energy gain when the HO−Sc{O(OH)$_2$}Sc−OH system (Figure 1i) is formed is 89 kJ/mol (S), and the product has C_{2v} symmetry. The central part of the system bears resemblance to ScO_3Sc, albeit the trigonal bipyramid is distorted due to the mismatch between the longer Sc···O bonds in the hydroxide bridges (2.11 Å (S)) and the short bond in the nearly right-angled Sc−O−Sc bridge (1.90 Å (S)). The addition reaction with the oxygen bridge in $(HO)_2ScOSc(OH)_2$(g) is exothermic by 12 kJ/mol using (S), but endothermic by 15 kJ/mol using (L). Both values must be considered small and define the precision of the present study. The $Sc(OH)_3$(g) product (Figure 1j) is planar, with open Sc−O−H bond angles (179° (S) and 164° (L)).

Although the additional stability of $(HO)ScO(OH)_2Sc(OH)$ efficiently suppresses fragmentation, water can react with the remaining Sc−O−Sc bridge. The product is the hydroxide $(HO)_2$>Sc<$(OH)_2$>Sc<$(OH)_2$ (Figure 1k), which has a planar $Sc(OH)_2Sc$ ring in the center and D_{2h} symmetry. The long Sc−O bonds (2.08 Å (S)) in conjunction with the rather unchanged O−Sc−O bond angle (80° (S)) make this ring more rhombohedrally distorted than that in $(HO)ScO_2Sc(OH)$(g). The terminal Sc−O bond lengths (1.86 Å (S)) and Sc−O−H bond angles (175° (S)) are similar to what was found for $(HO)ScO_2Sc(OH)$ above. The formation of $(HO)_2Sc(OH)_2Sc(OH)_2$ by water addition to $(HO)ScO(OH)_2Sc(OH)$(g) is exothermic by 224 kJ/mol (S), while the dimerization of two $Sc(OH)_3$(g) molecules is exothermic by 301 kJ/mol (S).

Further addition of a water molecule to the $Sc(OH)_3$(g) monomer to form the $Sc(OH)_3{\cdot}H_2O$(g) complex (Figure 1l) is exothermic by 121 kJ/mol (S).[4] While considerable, it should be noted that condensation of two such complexes into $(HO)_2Sc(OH)_2Sc(OH)_2$(g) is still exothermic by 59 kJ/mol (S). Furthermore, it is expected that the formation of hydrogen bonds between the dihydroxy-bridged aggregate and the two extra water molecules will release further energy,[4] thus making clustering even more favorable. Condensation of the terminal OH groups enables $Sc(OH)_2Sc$ rings to be interconnected by Sc−O−Sc bridges. This process is likely to be slightly exothermic when a 3D-network is formed, while it will be endothermic when strained polymeric chains with alternating ScO_2Sc and $Sc(OH)_2Sc$ rings are formed.

4.2. $Ti_2O_4 + 4H_2O$. The Ti_2O_4 molecule is the simplest binuclear oxide containing Ti(IV), with a central Ti_2O_2 ring and two terminal Ti═O bonds. When Ti_2O_4 is compared to the analogous Ge_2O_4,[3] the major difference is that while the latter system was found to be planar, O═Ti<O_2>Ti═O has a second-order saddle point in D_{2h} symmetry, and thus two minima where the Ti═O units are bent. The two structures differ in that the terminal oxygen arrangements can be cis (Figure 2a) or trans (Figure 2b). The latter structure is 27 kJ/mol (S) more stable than the former, and it is 103 kJ/mol (L) below the planar form. The Ti_2O_4 cluster can be understood as the dimer of TiO_2 (Figure 2c). The latter was used as the starting point for water addition in ref 4. The dimerization process comprises ring

formation matching two of the Ti═O bonds producing O═TiO_2-Ti═O is exothermic by 520 kJ/mol (S) and 477 kJ/mol (L). These energetics are similar to that observed for the formation of the (HO)ScO_2Sc(OH) ring cluster from two (HO)Sc═O molecules (cf. section 4.1).

There are two sites for water addition to OTiO_2TiO, being the Ti−O−Ti bridges in the ring and the terminal Ti═O bonds. Four different product routes are available for the reaction with the TiO_2Ti ring. The first route results in the HO−(O═Ti)−O−(Ti═O)−OH chain (Figure 2d), which adopts C_2 symmetry in its energy minimum. The Ti−O−Ti bridge is nearly linear (179° (S)), and the open Ti−O−H bond angles (151° (S)) suggest electrostatics to dominate the intramolecular fragment interactions. This is in contrast to the C_s minimum of the (HO)OGeOGeO(OH) chain, which displays an intramolecular hydrogen bond.[3] No such structure was found for the $Ti_2O_5H_2$ system. The addition reaction is exothermic by 167 kJ/mol (S).

The second route follows by a subsequent process, in which the remaining Ti−O−Ti bridge is bent, as the OH groups are used to form two Ti···(OH)···Ti bridges. The O═Ti{$O(OH)_2$}-Ti═O aggregate (Figure 2e) has C_s symmetry, and the Ti−O bond distances in the distorted central TiO_3Ti unit in the center are 1.86 Å (S) and 2.04 Å (S). This dihydroxy bridging stabilizes the system by 61 kJ/mol (S). An alternative stabilizing process, and third route, is the use of one Ti═O bond to form a rhombohedrally distorted TiO_2Ti ring. The resulting HO−Ti<O_2>Ti<O(OH) complex (Figure 2f) is 21 kJ/mol (S) below the oxyhydroxy triple-bridged system and has C_s symmetry. The long Ti···O complex bond (2.02 Å (S)) of the central TiO_2Ti ring can be associated with a description of the system as an (HO)TiO_2···$TiO(OH)^+$ complex.

Along the fourth route, both Ti═O bonds are used to form Ti−O−Ti bridges. The result is a symmetric triple-bridged central TiO_3Ti unit with two terminal OH groups. The linear Ti−O−H bond angles give the HO−Ti{O_3}Ti−OH cluster (Figure 2g) D_{3h} symmetry, as was found for ScO_3Sc (cf. section 4.1). The triple-bridged structure is 11 kJ/mol (S) more stable than the (HO)TiO_2TiO(OH) complex, and thus contrasting (HO)GeO_3Ge(OH), which was found to be of lower symmetry and the least stable configuration within the $Ge_2O_5H_2$ family.[3]

Finally, there is the route where water is added to one of the terminal Ti═O bonds, thus preserving the Ti_2O_2 ring. The O═Ti<O_2>Ti<$(OH)_2$(g) product (Figure 2h) has C_s symmetry, where the analogous OGeO_2Ge$(OH)_2$(g) has a planar configuration in the OGeO_2 subunit and C_2 symmetry.[3] Both structures are the most stable within their respective stoichiometries although OTiO_2Ti$(OH)_2$(g) is only 35 kJ/mol (S) below (HO)-TiO_3Ti(OH)(g). Consequently, the formation of OTiO_2Ti$(OH)_2$ from OTiO_2TiO(g) + H_2O is exothermic by 295 kJ/mol (S).

Dissociative addition of water to the Ti−O−Ti bridge in the (HO)OTiOTiO(OH) chain results in two O═Ti<$(OH)_2$ molecules (Figure 2m). This reaction is endothermic by 4 kJ/mol (S), and it seems plausible that the use of a larger basis set would slightly enhance the endothermicity. For reference, the alternative path for formation of Ti$O(OH)_2$(g), by water addition to TiO_2(g), was found exothermic by 341 kJ/mol (S) and 298 kJ/mol (L) per molecule.[3] This implies that the monomers will only release water by forming the more stable dimer clusters.

An alternative to bridge dissociation of the (HO)OTiOTiO-(OH) chain is water addition to one of the Ti═O bonds, which results in the formation of (HO)−(O═Ti)−O−Ti$(OH)_3$ (Figure 2i), while releasing 273 kJ/mol (S), consistent with the energetics of O═Ti═O + H_2O. The (HO)OTiOTi $(OH)_3$ chain possesses no symmetry elements and thus displays two enantiomers.

While water addition to one of the terminal Ti═O bonds in O$TiO(OH)_2$TiO is a second route to (HO)OTi−O−Ti$(OH)_3$, addition to the Ti−O−Ti bridge results in the HO(O═Ti)-<$(OH)_2$>(Ti═O)OH cluster. The C_{2v} structure (Figure 2j), which has the terminal OH groups cis, is the most stable one, whereas the C_{2h} structure (Figure 2k) with a trans arrangement lies 6 kJ/mol (S) higher. The 55 kJ/mol (S) stability of the former structure as compared to the chain determines the exothermicity for the hydrolysis of the Ti−O−Ti bridge in the O$TiO(OH)_2$TiO system to be 267 kJ/mol (S), which is due to the strained bonding.

A similar reactivity (272 kJ/mol (S)) is observed for adding water to one of the Ti−O−Ti bridges in the (HO)TiO_3Ti(OH) system. The product of the latter reaction is $(HO)_2$>Ti<O_2>Ti-<$(OH)_2$(g) (Figure 2l), which contains a central TiO_2Ti ring. This system can also be achieved by water reacting with the remaining Ti═O bond in OTiO_2Ti$(OH)_2$, releasing 307 kJ/mol (S), or by joining the Ti═O bonds in two O$Ti(OH)_2$ molecules, releasing 440 kJ/mol (S). It is also 107 kJ/mol (S) below the cis hydroxy-bridged (HO)OTi$(OH)_2$TiO(OH) cluster.

Two types of polymeric structures can be formed by aggregation of $(HO)_2TiO_2Ti(OH)_2$ monomers, via condensation of OH groups. The first type comprises the formation of TiO_2-Ti rings, and this gives the $(>Ti<O_2>)_n$ double chains, whereas the second type utilizes the out-of-plane direction to connect the TiO_2Ti ring by one or two Ti−O−Ti bridges to other rings. This bonding is less strained and may be used as a strategy for making supramolecular solids.

While hydrolysis of the Ti−O−Ti bridge in the (HO)OTiOTi-$(OH)_3$ chain is slightly endothermic (13 kJ/mol (S)), water addition to the Ti═O bond is exothermic by 269 kJ/mol (S). The $(HO)_3$Ti−O−Ti$(OH)_3$(g) product (Figure 2o) has a linear Ti−O−Ti bridge and linear Ti−O−H bond angles, which together with a nearly tetrahedral oxygen coordination at the Ti atom produce an energy minimum of D_3 symmetry. Subsequent hydrolysis of the oxygen bridge, forming two Ti-$(OH)_4$(g) molecules (Figure 2p), is endothermic by 17 kJ/mol (S). Forming the same species by water addition to Ti$(OH)_2$-(g) was found exothermic by 269 kJ/mol (S) per reactant.[4] It is noted that this reactivity of the Ti═O bond in Ti$(OH)_2$ is, somewhat fortuitously, identical to that of (HO)OTiOTi$(OH)_3$. This similarity demonstrates the efficiency of a qualitative local chemical understanding of the systems at hand.

Adding water to one of the Ti−O−Ti bridges in $(HO)_2TiO_2$-Ti$(OH)_2$(g) also produces $(HO)_3$TiOTi$(OH)_3$(g), and this reaction is exothermic by 114 k/mol (S). For this reaction, a competing product is an isomer to the D_3 structure of $(HO)_3$TiOTi$(OH)_3$, which analogously to $(HO)_3$GeOGe$(OH)_3$(g) has two intramolecular hydrogen bonds (Figure 2n).[3] While it is found that this isomer is 17 kJ/mol (S) less stable than the D_3 structure, it could still be argued that the hydrogen-bonded species may prove more interesting due to its conformation, which allows for reversible hydrolysis and water condensation.

In excess of water, Ti$(OH)_4$ is expected to be further stabilized by the energy gain from solvation. This effect is expected to alter the energy balance for hydrolysis of the remaining Ti−O−Ti bridge in favor of the latter species. The fact that Ti-$(OH)_4$(aq) is the final product at low Ti concentrations implies that it is not the strengths of the chemical bonds that determine the protective properties of titanium oxide toward corrosion. Rather, it is the spatial tightness of the oxide which prevents it from deteriorating under humid conditions.

Table 3. Summaries of Bond Lengths R (Å) and Bond Angles A (deg), and Ranges of Vibrational Frequencies (cm^{-1}), Together with Normal Mode Symmetries and the Number of Vibrations in Each Group, for the V Systems

O_2VOVO_2

C_{2v}	R(V═O): 1.587	A(O═V═O): 110.2	A(V−O−V): 162.8
(S)	R(V−O): 1.789	A(O═V−O): 115.8	
	A_2 (1 vib): 50*i*		
	$A_1 + A_2 + B_1 + B_2$ (5+2+3+4 vib): 51−1092		
C_{2v}	R(V═O): 1.589	A(O═V═O): 111.5	A(V−O−V): 164.6
(L)	R(V−O): 1.805	A(O═V−O): 118.3	
	A_2 (1 vib): 49*i*		
	$A_1 + A_2 + B_1 + B_2$ (5+2+3+4 vib): 32−1071		
C_2	R(V═O): 1.587−1.589	A(O═V═O): 110.7	A(V−O−V): 166.1
(S)	R(V−O): 1.784	A(O═V−O): 114.3−115.8	
	A + B (6+4 vib): 39−491		
	A + B (2+3 vib): 969−1092		
C_2	R(V═O): 1.587−1.589	A(O═V═O): 111.5	A(V−O−V): 164.6
(L)	R(V−O): 1.799	A(O═V−O): 117.1−118.4	
	A + B (6+4 vib): 43−482		
	A + B (2+3 vib): 923−1085		

OVO_3VO

D_{3h}	R(V═O): 1.575	A(O═V−O): 128.5	A(V−O−V): 77.0
(S)	R(V−O): 1.835	A(O−V−O): 85.4	
	E″ (1 vib): 196*i*		
	$A_1' + A_2'' + E' + E''$ (2+1+3+1 vib): 157−797		
	$A_1' + A_2''$ (1+1 vib): 1107−1145		

OVO_2VO_2

C_s	R(V···O): 1.979	A(O═V═O): 94.0−113.0	A(V═O···V): 94.3−118.2
(S)	R(V═O): 1.579−1.691	A(O···V···O): 77.3	
	A′ + A″ (6+4 vib): 83−591		
	A′ + A″ (1+1 vib): 850−915		
	A′ (3 vib): 1081−1111		

$O_2VOVO(OH)_2$

C_s	R(V═O): 1.573−1.589	A(V−O−H): 137.3	A(V−O−V): 168.8
(S)	R(V−O): 1.754−1.781	A(O−V−O): 109.7−110.2	A(O═V═O): 110.6
	R(O−H): 0.965		A(O═V−O): 108.5−115.7
	A′ + A″ (10+8 vib): 33−862		
	A′ + A″ (3+1 vib): 968−1114		
	A′ + A″ (1+1 vib): 3802−3806		

$O_2V(OH)_2VO_2$

D_{2h}	R(V═O): 1.582	A(V···O−H): 130.9	A(V···O···V): 98.1
(S)	R(V···O): 1.960	A(O···V···O): 81.9	A(O═V═O): 109.3
	R(O−H): 0.964		A(O═V···O): 115.9
	$A_{g/u} + B_{1g/u} + B_{2g/u} + B_{3g/u}$ (5+4+7+6 vib): 59−1109		
	$A_g + B_{1u}$ (1+1 vib): 3831−3832		

$O_2VO_2V(OH)_2$

C_{2v}	R(V═O): 1.586−1.681	A(V−O−H): 151.9	A(V═OV): 95.2
(S)	R(V−O): 1.728	A(O−V−O): 112.2	A(O═V═O): 93.1−111.5
	R(V···O): 1.971	A(O···V···O): 76.5	A(O═V−O): 112.6
	R(O−H): 0.963		A(O═V···O): 116.2
	$A_1 + A_2 + B_1 + B_2$ (8+3+5+6 vib): 65−1098		
	$A_1 + B_2$ (1+1 vib): 3848−3854		

$(HO)OVO_2VO(OH)$

C_{2v}	R(V═O): 1.571	A(V−O−H): 143.6	A(V−O−V): 94.9
(S)	R(V−O): 1.743−1.799	A(O−V−O): 85.1−115.8	A(O═V−O): 112.0−113.2
	R(O−H): 0.964		
	$A_1 + A_2 + B_1 + B_2$ (8+4+4+6 vib): 79−1132		
	$A_1 + B_2$ (1+1 vib): 3821−3823		
C_{2h}	R(V═O): 1.571	A(V−O−H): 144.2	A(V−O−V): 95.0
(S)	R(V−O): 1.743−1.800	A(O−V−O): 85.0−116.0	A(O═V−O): 111.8−113.3
	R(O−H): 0.964		
	$A_g + A_u + B_g + B_u$ (7+4+4+7 vib): 79−1123		
	$A_g + B_u$ (1+1 vib): 3822−3824		

$(HO)_2OVOVO(OH)_2$

C_2	R(V═O): 1.570	A(V−O−H): 122.1−133.4	A(V−O−V): 117.8
(S)	R(V−O): 1.748−1.788	A(V−O···H): 105.8	A(O═V−O): 110.7−114.3
	R(O−H): 0.967−0.984	A(H−O···H): 122.3	A(O−V−O): 103.7−110.0
	R(O···H): 2.045		A(O−H−O): 136.7
	A + B (14+13 vib): 60−877		
	A + B (1+1 vib): 1120−1138		
	A + B (2+2 vib): 3504−3784		
C_{2v}	R(V═O): 1.575	A(V−O−H): 137.5	A(V−O−V): 168.9
(S)	R(V−O): 1.754−1.767	A(O−V−O): 110.0−110.6	A(O═V−O): 108.7−108.8
	R(O−H): 0.965		
	A_2 (1 vib): 22*i*		
	$A_1 + A_2 + B_1 + B_2$ (9+6+6+8 vib): 42−1114		
	$A_1 + A_2 + B_1 + B_2$ (1+1+1+1 vib): 3803−3809		
C_2	R(V═O): 1.575	A(V−O−H): 137.3−137.6	A(V−O−V): 172.3
(S)	R(V−O): 1.753−1.766	A(O−V−O): 109.1−110.2	A(O═V−O): 108.3−109.1
	R(O−H): 0.965		
	A + B (12+10 vib): 23−569		
	A + B (3+4 vib): 780−1111		
	A + B (2+2 vib): 3803−3809		

$VO_2(OH)$

C_1	R(V═O): 1.589−1.590	R(O−H): 0.960	A(O═V═O): 110.3
(S)	R(V−O): 1.759	A(V−O−H): 155.7	A(O═V−O): 116.2−117.1
	A (6 vib): 136−828		
	A (2 vib): 1083−1086		
	A (1 vib): 3887		
C_1	R(V═O): 1.589−1.590	R(O−H): 0.962	A(O═V═O): 112.3
(L)	R(V−O): 1.794	A(V−O−H): 125.8	A(O═V−O): 116.7−118.7
	A (6 vib): 159−758		
	A (2 vib): 1075−1079		
	A (1 vib): 3860		

$VO(OH)_3$

C_{3v}	R(V═O): 1.575	R(O−H): 0.965	A(O═V−O): 108.7
(S)	R(V−O): 1.757	A(V−O−H): 137.3	A(O−V−O): 110.3
	$A_1 + E$ (4+5 vib): 242−1110	$A_1 + E$ (2+1 vib): 3806−3813	
C_{3v}	R(V═O): 1.569	R(O−H): 0.962	A(O═V−O): 109.4
(L)	R(V−O): 1.778	A(V−O−H): 122.5	A(O−V−O): 109.6
	$A_1 + E$ (4+5 vib): 235−1115		
	$A_1 + E$ (2+1 vib): 3859−3866		

4.3. $V_2O_5 + 3H_2O$. The O_2>V−O−V<O_2 molecule (Figure 3a) is the binuclear vanadium oxide system primarily employed for modeling the reactions of a V_2O_5(s) prototype with water. It is similar to O═Sc−O−Sc═O in having one oxygen bridge, while the two V═O bonds on each V stabilize this chain toward further clustering. Rotation of the VO_2 units around the V−O−V bridge results in a local energy minimum of C_2 symmetry. The V−O−V bond angle is quite open (166° (S) and 165° (L)), and each V atom has a slightly pyramidal oxygen environment.

It is possible to improve the V−O interactions by forming a structure similar to that in ScO_3Sc(g). While the O═V{O_3}V═O structure (Figure 3b) is a second-order saddle point in D_{3h} symmetry, it is still 23 kJ/mol (S) more stable than O_2VOVO_2. The global minimum of the V_2O_5 system is an O_2>V<O_2>V═O(g) complex (Figure 3c) with C_s symmetry. It can be understood as an ion pair, i.e. consisting of an O_2>V^+ cation and an $^-O_2$>V═O anion. While the three V═O bonds are normal (1.58−1.59 Å (S)), the central VO_2V ring displays two long (1.98 Å (S)) and two short (1.69 Å (S)) V−O bonds. The shape of the VO_2V ring is accordingly distorted, with an acute O−V−O bond angle (77° (S)) and more open angle (94° (S)) associated with the long and short V−O bonds, respectively.

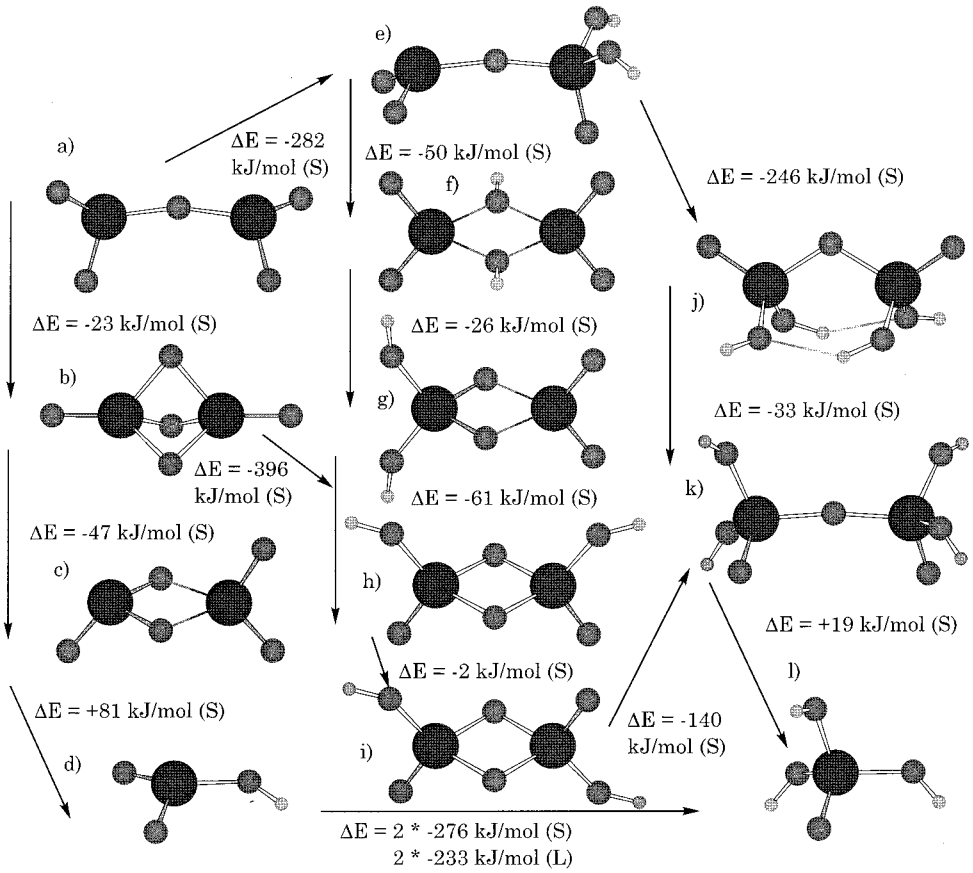

Figure 3. Structures in the $V_2O_5 + 3H_2O$ system together with relative stabilities and energetics for some hydrolysis reactions. V_2O_5: (a) O_2VOVO_2 (C_2), (b) OVO_3VO (D_{3h}), (c) OVO_2VO_2 (C_s). $V_2O_6H_2$: (d) $2VO_2(OH)$ (C_1), (e) $O_2VOVO(OH)_2$ (C_s), (f) $O_2V(OH)_2VO_2$ (D_{2h}), (g) $O_2VO_2V(OH)_2$ (C_{2v}), (h) $(HO)OVO_2VO(OH)$ (C_{2v}), (i) $(HO)OVO_2VO(OH)$ (C_{2h}). $V_2O_7H_4$: (j) $(HO)_2OVOVO(OH)_2$ (C_2), (k) $(HO)_2OVOVO(OH)_2$ (C_2), (l) $2VO(OH)_3$ (C_{3v}).

The O_2VO_2VO complex is 47 kJ/mol (S) more stable than the OVO_3VO cluster, and 70 kJ/mol (S) more stable than the O_2VOVO_2 chain.

The V−O−V bridge in O_2VOVO_2(g) constitutes one proper model for dissociative addition of water. In this process, two O_2>V−OH molecules (Figure 3d) are formed, and the reaction is endothermic by 11 kJ/mol (S) and 24 kJ/mol (L). The effect of increasing the basis set on reactivities is thus smaller (13 kJ/mol) than what has previously been observed (∼30 kJ/mol), but the sign on the correction persists.

The formation of O_2>V−O−(V═O)<$(OH)_2$ (Figure 3e) by adding water to a V═O bond in O_2VOVO_2 is exothermic by 282 kJ/mol (S). The structure has C_s symmetry and preserves the wide V−O−V angle (169° (S)) found for O_2VOVO_2. A second route to this structure is achieved by water addition to the VO_2V ring in O_2VO_2VO. This reaction is somewhat less exothermic, 212 kJ/mol (S). An alternative conformation is reached if allowing for a central ring containing two V···(OH)···V bridges. This O_2>V<$(OH)_2$>V<O_2 cluster (Figure 3f) has D_{2h} symmetry, and it is 50 kJ/mol (S) more stable than the $O_2VOVO(OH)_2$ chain. The V···O bond distances 1.96 Å (S) in the central ring are similar to those seen for the O_2VO_2VO complex above. This $O_2V(OH)_2VO_2$ cluster is stable by 343 kJ/mol (S) toward dissociation into two VO_2(OH) monomers.

Water addition to one of the terminal V═O bonds in the O_2VO_2VO complex produces the O_2>V<O_2>V<$(OH)_2$ complex (Figure 3g). The fact that the distorted VO_2V ring is preserved stabilizes the system by an additional 26 kJ/mol (S) as compared to $O_2V(OH)_2VO_2$. Further stabilization is achieved when going to the (HO)O>V<O_2>V<O(OH) system. There are two isomeric conformations for this cluster: cis (Figure 3h), with C_{2v} symmetry, and trans (Figure 3i), with C_{2h} symmetry. The latter structure is 2 kJ/mol (S) below the former and 64 kJ/mol (S) more stable than the $O_2VO_2V(OH)_2$ complex. Given that the C_{2v} structure also constitutes the product of water addition to one of the V−O−V bridges in the OVO_3VO model cluster, it is noted that this reaction is exothermic by 396 kJ/mol (S). Finally, clustering of two VO_2(OH)(g) molecules into the C_{2v} structure, using one V═O bond on each monomer to form the VO_2V ring, is exothermic by 432 kJ/mol (S). Polymerization of $(HO)OVO_2VO(OH)$ by condensation is expected to produce a $(V_2O_5)_n$ chain by connecting OVO_2VO units via V−O−V bridges.

Water addition to one of the V═O bonds in the remaining VO_2 unit in $O_2VOVO(OH)_2$ results in the $(HO)_2$>(O═V)-O−(V═O)<$(OH)_2$ chain (Figure 3k), and the reaction is exothermic by 279 kJ/mol (S). Each of the V atoms in the chain is positioned in a slightly distorted tetrahedral oxygen environment, including one V═O bond (1.58 Å (S)), two V−OH bonds (1.75 Å (S)), and a nearly linear V−O−V bridge (172° (S)) with a 1.77 Å (S) V−O bond distance. Rotation of the terminal $O(OH)_2$ group on one V into a staggered configuration relative to the group on the other V atom results in an energy minimum of C_2 symmetry. The structure resembles the O_2VOVO_2 chain and differs only in that one V═O group is replaced by two V−OH groups on each V. Condensation of the OH groups provides one way to understand the V_2O_5(s) bulk material.

The chain structure can also be formed from $(HO)OVO_2VO(OH)$ by adding water to the central VO_2V ring. Indeed, reaction with the C_{2h} structure is exothermic by 140 kJ/mol (S).

Table 4. Summaries of Bond Lengths R (Å) and Bond Angles A (deg), and Ranges of Vibrational Frequencies (cm^{-1}), Together with Normal Mode Symmetries and the Number of Vibrations in Each Group, for the Cr/OH Systems

		$O_2CrO_2CrO_2$	
D_{2h}	R(Cr═O): 1.558	A(O−Cr−O): 86.0	A(Cr−O−Cr): 94.0
(S)	R(Cr−O): 1.778	A(O═Cr−O): 114.4	A(O═Cr═O): 111.2
		$A_{g/u} + B_{1g/u} + B_{2g/u} + B_{3g/u}$ (5+4+5+4 vib): 78−1133	
		$(HO)O_2CrOCrO_2(OH)$	
C_{2v}	R(Cr═O): 1.565	A(Cr−O−H): 141.9	A(Cr−O−Cr): 165.9
(S)	R(Cr−O): 1.721−1.742	A(O−Cr−O): 109.3	A(O═Cr═O): 107.8
	R(O−H): 0.965		A(O═Cr−O): 109.6
$A_2 + B_1$ (2+1 vib): 236i−16i		$A_1 + A_2 + B_1 + B_2$ (8+5+5+7 vib): 38−1100	
		$A_1 + B_2$ (1+1 vib): 3813−3815	
C_2	R(Cr−O): 1.740−1.732	A(Cr−O−H): 130.2	A(Cr−O−Cr): 171.9
(S)	R(Cr═O): 1.563−1.564	A(O−Cr−O): 109.8	A(O═Cr═O): 109.7
	R(O−H): 0.970		A(O═Cr−O): 109.1−109.6
A + B (10+8 vib): 17−619		A + B (3+4 vib): 821−1109	
		A + B (1+1 vib): 3743−3744	
		CrO_3	
C_{3v}	R(Cr═O): 1.578	A(O═Cr═O): 113.2	
(S)	$A_1 + E$ (1+1 vib): 302−402	$A_1 + E$ (1+1 vib): 1024−1095	
C_{3v}	R(Cr═O): 1.576	A(O═Cr═O): 114.8	
(L)	$A_1 + E$ (1+1 vib): 244−386	$A_1 + E$ (1+1 vib): 1018−1090	
		$CrO_2(OH)_2$	
C_2	R(Cr═O): 1.565	R(O−H): 0.970	A(O═Cr═O): 110.4
(S)	R(Cr−O): 1.739	A(Cr−O−H): 128.5	A(O═Cr−O): 108.4−109.4
			A(O−Cr−O): 110.0
A + B (7+6 vib): 217−1114		A + B (1+1 vib): 3740−3745	

Table 5. Summaries of Bond Lengths R (Å) and Bond Angles A (deg), and Ranges of Vibrational Frequencies (cm^{-1}), Together with Normal Mode Symmetries and the Number of Vibrations in Each Group, for the Cr/F Systems

		$FO_2CrOCrO_2F$	
C_{2v}	R(Cr═O): 1.556	A(O−Cr−F): 109.8	A(Cr−O−Cr): 168.8
(S)	R(Cr−O): 1.738	A(O═Cr−O): 109.6	A(O═Cr═O): 108.4
	R(Cr−F): 1.715	A(O═Cr−F): 109.6	
	A_2 (1 vib): 41i	$A_1 + A_2 + B_1 + B_2$ (7+4+4+5 vib): 39−1119	
C_2	R(Cr═O): 1.556−1.557	A(O−Cr−F): 109.8	A(Cr−O−Cr): 168.9
(S)	R(Cr−O): 1.737	A(O═Cr−O): 109.5−109.7	A(O═Cr═O): 108.7
	R(Cr−F): 1.716	A(O═Cr−F): 109.4−109.8	
A + B (8+6 vib): 19−514		A + B (1+2 vib): 772−991	
		A + B (3+1 vib): 1098−1119	
		$CrFO_2(OH)$	
C_1	R(Cr═O): 1.559	R(O−H): 0.969	A(O═Cr═O): 109.2
(S)	R(Cr−O): 1.723	A(Cr−O−H): 132.9	A(O═Cr−O): 109.4−109.8
	R(Cr−F): 1.723	A(O−Cr−F): 109.7	A(O═Cr−F): 109.0−109.7
A (6 vib): 241−436		A (3 vib): 603−857	
		A (3 vib): 1103−3757	
		CrF_2O_2	
C_{2v}	R(Cr═O): 1.553	A(F−Cr−F): 110.0	A(O═Cr═O): 108.5
(S)	R(Cr−F): 1.711		A(O═Cr−F): 109.6
		$A_1 + A_2 + B_1 + B_2$ (2+1+1+1 vib): 224−436	
		$A_1 + B_1 + B_2$ (2+1+1 vib): 758−1128	

If a chain structure of $(HO)_2OVOVO(OH)_2$ with *intramolecular hydrogen bonds* is sought (Figure 3j), then water addition to the cis structure should be chosen. This reaction is exothermic by 109 kJ/mol (S), while the hydrogen-bonded chain is 33 kJ/mol (S) above the open chain. This structure has C_2 symmetry and displays two enantiomers, where each form is stabilized from rotation into its mirror structure by the hydrogen bonding.

The V−O−V bridge in the open isomer of $(HO)_2OVOVO(OH)_2$ constitutes an ideal model for M−O−M hydrolysis. The formation of O═V{$(OH)_3$ (Figure 3l) is found to be endothermic by 19 kJ/mol (S), and the use of a larger basis set is expected to stabilize further the binuclear system. For reference, water addition to $VO_2(OH)$, resulting in $VO(OH)_3$(g), was found exothermic by 276 kJ/mol (S) and 233 kJ/mol (L),[4] whereas further addition of water was found quite endothermic. Thus $V(OH)_5$(g) was concluded not to be a likely product even at humid conditions. Rather, the formation of hydrogen-bonded water complexes, eventually producing the solvated $VO(OH)_3$(aq), is implied.[4] This reaction product would be sufficiently stable to be competitive as compared to $(HO)_2OVOVO(OH)_2$.

4.4. $Cr_2O_6 + 2H_2O$ and $Cr_2O_6 + 4HF$. One main objective of the present investigation was to add further chemical understanding as to how the protective chromium oxide scale on chromium-alloyed steels deteriorates in the presence of water vapor at elevated temperatures. Experiment has suggested formation of hypothesized $CrO_2(OH)_2$(g) to be the main channel for loss of chromium.[2] Indeed, the condensation product in the cooler region of the furnace partly contained Cr(VI). It is envisaged that Cr_2O_3(s) is the dominant component at the steel surface, and that Cr(VI) is formed by a concerted oxidation and hydrolysis process. Thus $(CrO_3)_n$ chain transients, i.e. nanodomains of CrO_3(s), are formed from which $CrO_2(OH)_2$(g) is understood to evaporate under humid conditions. The present investigation serves two purposes in this context. First, the stability of the $-O-(CrO_2)-O-(CrO_2)-$ chain toward hydrolysis, which is critical for the evaporation process, is addressed. Second, possible reverse processes are considered, whereby two $CrO_2(OH)_2$(g) molecules (a) condense to form $HO-(O_2Cr)-O-(CrO_2)-OH$ and (b) emit a second H_2O molecule to form $O_2Cr<O_2>CrO_2$ in the gas phase. The energetics of the latter reactions determine to some extent which forms of Cr(VI) will eventually condense on the cold parts of the furnace.

The natural starting point for this investigation comprises the $O_2>Cr<O_2>Cr<O_2$ cluster (Figure 4a). It can be understood to form by dimerization of two CrO_3 molecules (Figure 4b). Thus, there are two terminal Cr═O bonds on each Cr atom, while these atoms are connected via a central CrO_2Cr ring. The

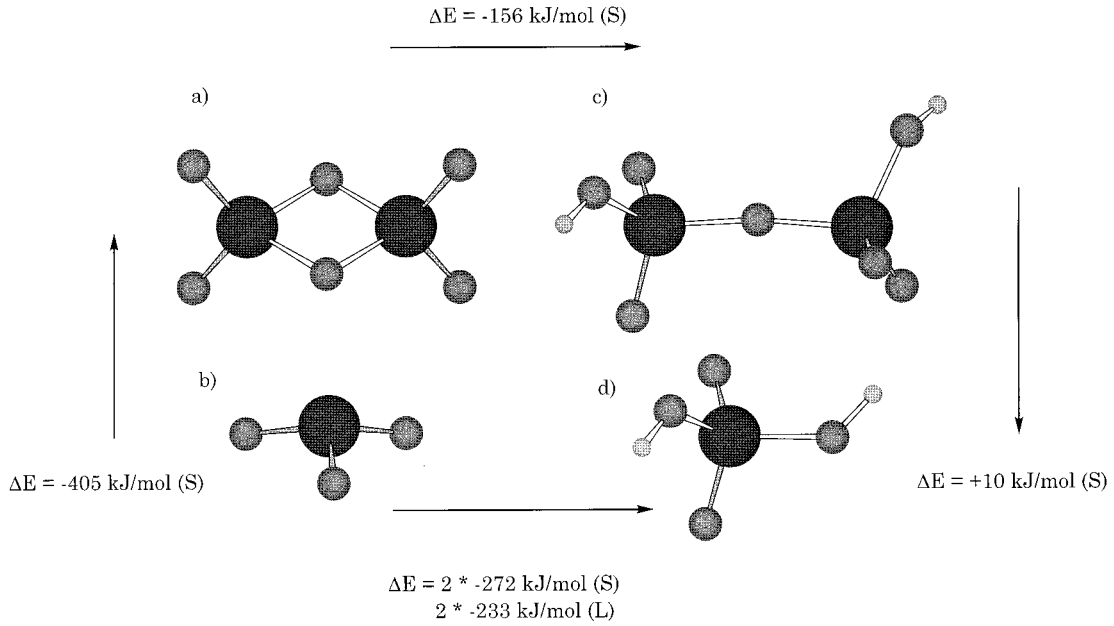

Figure 4. Structures in the $Cr_2O_6 + 2H_2O$ system together with relative stabilities and energetics for the hydrolysis reactions. Cr_2O_6: (a) O_2CrO_2-CrO_2 (D_{2h}), (b) $2CrO_3$ (C_{3v}). $Cr_2O_7H_2$: (c) $(HO)O_2CrOCrO_2(OH)$ (C_2). $Cr_2O_8H_4$: (d) $2CrO_2(OH)_2$ (C_2).

cluster formation is exothermic by 405 kJ/mol (S). This reactivity is in general agreement with what was found previously when employing two M═O bonds to form a MO_2M ring (vide supra).

Given that water addition to an M═O terminal bond is beneficial only if the resulting number of oxygens directly associated with the central metal atom is less than 5, hydrolysis is expected to occur at one of the Cr−O−Cr bridges in the ring. The product is the $(HO)O_2Cr-O-CrO_2(OH)$ chain (Figure 4c), in which the Cr−O−Cr bridge is nearly linear (172° (S)). Thus, this chain structure is very similar to that of $(HO)_2OVOVO(OH)_2$ (cf. section 4.3), replacing one V−OH by Cr═O. Condensation of the terminal Cr−OH groups in $(HO)O_2CrOCrO_2(OH)$ results in a $(CrO_3)_n$ chain, composed of CrO_4 tetrahedra. Such a structure is known to be the characteristic component in bulk CrO_3(s).[13,14]

The subsequent water-induced dissociation of the Cr−O−Cr bridge in the chain structure is found to be endothermic by 10 kJ/mol (S), while an improved basis set better is expected to increase this endothermicity by 10−30 kJ/mol. However, in order to react with the bridge, the oxygen in the water molecule has to coordinate to one of the Cr atoms, implying a five-coordinated transition state for hydrolysis. The activation energy for such a reaction will be decisive for the hydrolysis, and a value of at least 84 kJ/mol can be estimated from the TS for the addition reaction $CrO_2(OH)_2 + H_2O$.[4]

The water addition produces two $(HO)_2>Cr<O_2$ molecules (Figure 4d), for which a C_s and a C_2 minimum was found, resulting from different orientation of the OH groups.[4] The latter structure was found to be slightly more stable than the former. The direct formation of this species from CrO_3(g) was investigated in detail, initially forming an M−O bonded water complex, followed by a TS and a 108 kJ/mol (S) energy barrier for the hydrolysis step, and finally the $CrO_2(OH)_2$ product.[4] The total reaction was found exothermic by 272 kJ/mol (S) and 233 kJ/mol (L), and the excess energy from the initial complex formation is sufficient to surpass the barrier. However, rather than adding further H_2O to the remaining Cr═O bonds, $CrO_2(OH)_2$(g) was found to form hydrogen-bonded complexes with water. The final product is the solvated molecule,[4] which competes efficiently with the chain structure. It is concluded that the limited accessibility of water to Cr in the $-O-(CrO_2)-O-$ tetrahedra is the decisive factor, controlling the dissociative water addition to the bridge.

In order to test the qualitative validity of a truncated model chain, the terminal OH groups were replaced by flourides, and energetics and structures were computed and compared to what was obtained for OH termination. Experimentally observed accelerated erosion of the protective chromium oxide scale by the presence of HCl(g) in the humid reaction atmosphere comprises a further incentive for addressing the HF(g) chemistry.[5]

The chemistry of CrO_3(s) with HF(g) is integrated in the present scheme, by formulating model reactions where either one Cr−OH and one Cr−F group or two Cr−F and one H_2O(g) are produced. Consequently, addition of two HF molecules to $O_2>Cr<O_2>Cr<O_2$ produces the $F-(O_2Cr)-O-(CrO_2)-F$ chain (Figure 5a) and a water molecule. Similar to the hydroxide chain, the energy minimum for the flouride analogue has C_2 symmetry. The exothermicity for this reaction becomes 184 kJ/mol (S), and the product structure is strikingly similar to the OH truncated analogue.

An increased degree of flourination leads to a marginally though significant increase in reactivity, as can be seen from the following sequence. Adding one H_2O to $FO_2CrOCrO_2F$ produces two $(HO)F>Cr<O_2$ molecules (Figure 5b), and the reaction is endothermic by 1 kJ/mol. Using one HF molecule to dissociate the Cr−O−Cr bridge produces one $CrFO_2(OH)$ and one $F_2>Cr<O_2$ (Figure 5c), which is exothermic by 7 kJ/mol (S). If two HF(g) are used, and two CrF_2O_2 and one H_2O are produced, the exothermicity increases to 17 kJ/mol (S). Finally, in the reaction between one CrO_3 molecule and one HF, forming $CrFO_2(OH)$ is exothermic by 294 kJ/mol (S), while the reaction with two HF, forming one CrF_2O_2(g) and one H_2O(g), is exothermic by 303 kJ/mol (S). Thus a 31 kJ/mol (S) increase of the exothermicity for this process is noted, as compared to adding one H_2O(g).

It can be concluded from the above that deterioration of CrO_3(s) requires a moist atmosphere to become exothermic, as $CrO_2(OH)_2$(g) and $(HO)O_2CrOCrO_2(OH)$(g) become the competitive

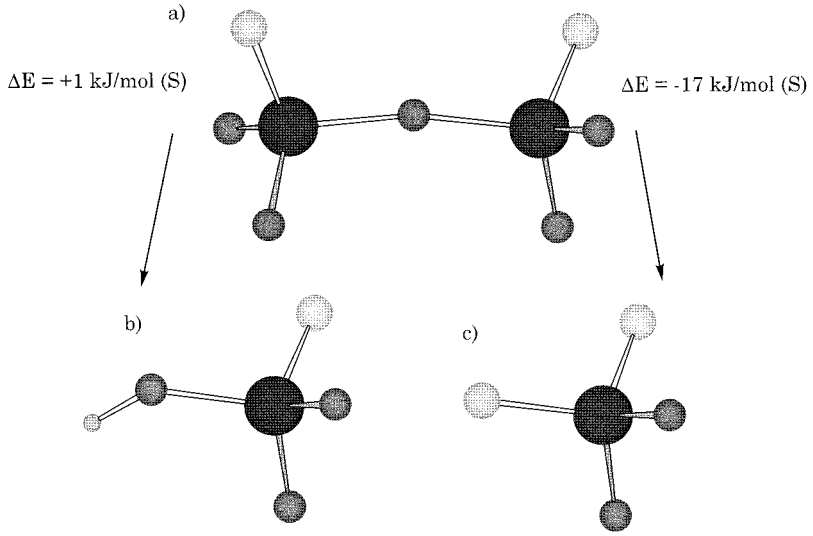

Figure 5. Flouride structures in the $Cr_2O_6 + 4HF$ system together with energetics for the hydrolysis and hydroflourination reactions. $Cr_2O_5F_2$: (a) $F(O_2Cr)O(CrO_2)F$ (C_2). $Cr_2O_6F_2H_2$: (b) $2CrO_2F(OH)$ (C_1). $Cr_2O_4F_4$: (c) $2CrO_2F_2$ (C_{2v}).

Table 6. Summaries of Bond Lengths R (Å) and Bond Angles A (deg), and Ranges of Vibrational Frequencies (cm^{-1}), Together with Normal Mode Symmetries and the Number of Vibrations in Each Group, for the Mn Systems

		$O_3MnOMnO_3$	
C_{2v}	R_1(Mn−O_1): 1.729	A_4(O_2−Mn−O_3): 110.5	A_1(Mn−O_1−Mn): 154.7
(S)	R_2(Mn−O_2): 1.564	A_5(O_3−Mn−O_3): 110.1	A_2(O_1−Mn−O_2): 108.3
	R_3(Mn−O_3): 1.564		A_3(O_1−Mn−O_3): 108.7
		$A_1 + A_2 + B_1 + B_2$ (5+3+3+3 vib): 29−525	
		$A_1 + A_2 + B_1 + B_2$ (2+1+1+3 vib): 959−1072	
		$MnO_3(OH)$	
C_s	R(Mn═O): 1.563−1.566	R(O−H): 0.974	A(O═Mn═O): 109.6−111.2
(S)	R(Mn−O): 1.733	A(Mn−O−H): 122.9	A(O═Mn−O): 106.6−109.0
A′ + A″ (7+4 vib): 208−1079		A′ (1 vib): 3680	

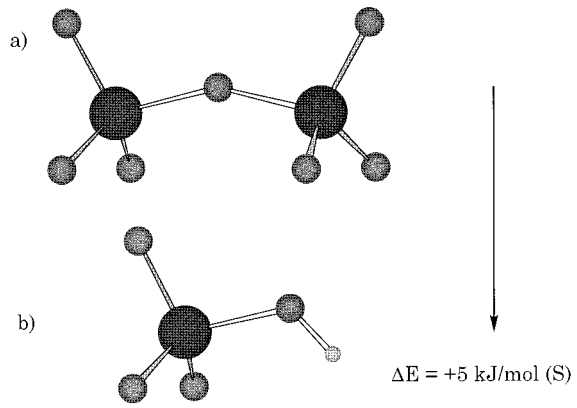

Figure 6. Structures in the $Mn_2O_7 + H_2O$ system together with energetics for the hydrolysis reaction. Mn_2O_7: (a) $O_3MnOMnO_3$ (C_{2v}). $Mn_2O_8H_2$: (b) $2MnO_3(OH)$ (C_s).

products. In general, the reactivity toward hydrolysis of the single Cr−O−Cr bridge is modest, whereas HF(g) is found to be a more efficient "cutting tool".

4.5. $Mn_2O_7 + H_2O$. Similar to CrO_3(s), the metal atoms in the molecular permanganic acid anhydride, Mn_2O_7, are positioned in the center of oxygen tetrahedra. The three terminal Mn═O bonds on each metal ion exclude any chain formation, and the molecular solid is formed from these binuclear oxide monomers, which preserve their molecular identity in the bulk material.[13] The minimum structure of the $O_3Mn-O-MnO_3$ molecule (Figure 6a) has C_{2v} symmetry. Although the oxygen configuration on Mn is nearly tetrahedral, the Mn−O−Mn bridge is slightly bent (155° (S)). The interactions between the nonbonding orbitals of the bridging O atom and the MnO_3 units stabilize the eclipsed structure of $O_3MnOMnO_3$.

Water addition to the oxygen bridge in $O_3MnOMnO_3$ results in two permanganic acid molecules, O_3Mn-OH (Figure 6b), and the reaction is endothermic by 5 kJ/mol (S). The potential energy surface of $MnO_3(OH)$(g) has three equivalent energy minima of C_s symmetry, in which the OH group has a staggered position, with respect to the Mn═O units. The eclipsed conformations, which also have C_s symmetry, are transition states. Further addition of water to $MnO_3(OH)$(g) is possible, but was found to be rather endothermic for one H_2O(g), while adding a second water molecule resulted in a collapsed peroxide structure.[4] Formation of hydrogen-bonded complexes with water is favorable for $MnO_3(OH)$, similar to what was seen for $VO(OH)_3$ and $CrO_2(OH)_2$.

4.6. M−O Distances in the Transition Metal Oxide Systems. The rich variety of transition metal oxide structures originates from their ability to form single and multiple bonds to oxygen, which competes in the bulk with simple ionic stacking. Investigations based on cluster calculations assume that local interactions dominate, and hence that chemical effects are decisive for the structure. Thus, it is expected that the cluster model approach to the oxygen coordination of transition metals should apply for disordered systems, for molecular crystals, for low-dimensional systems such as polymers, and at surfaces. Also, a more detailed analysis reveals that locality dominates for systems, which display high oxidation states and low coordinations on the metal, e.g. tetrahedral coordination at an oxidation state greater than +4 implies at least one local M═O bond. Thus chemical bonding becomes a decisive local property for understanding the bulk structure.

The semiquantitative validity of such a local understanding of the M−O bonds for bulk systems is seen on inspection of Figure 7. Averaged bond distances, from B3LYP transition

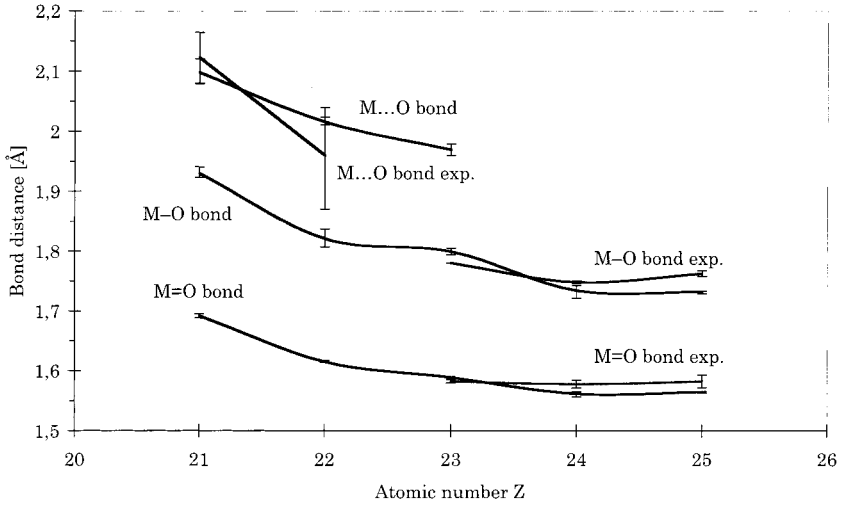

Figure 7. M−O bond distance as function of *Z* for complex, single, and double bonds, as determined by calculations and crystallography.[15] The error bars, one for each type of M−O bond and *Z*, indicate the distribution of bond distances.

metal structures in this work, are plotted against the atomic number *Z*. All three bond types, single M−O, multiple M═O, and complex M···O, e.g., M···(OH)···M, are included. It is gratifying to note the close agreement in magnitudes and trends, when comparison is made to relevant experimental data,[15] and this agreement demonstrates the degree to which the molecular approach is applicable.

5. Concluding Remarks

The water chemistry of binuclear transition metal oxide molecules has been investigated. Stabilities of single, double, and triple M−O−M bridges to hydrolysis were studied. Consecutive addition was considered, resulting in mononuclear oxyhydroxides and hydroxides, the stabilities of which were investigated in a previous study.[4] The structures of a menagerie of molecular binuclear transition metal oxides, oxyhydroxides, and hydroxides were determined, and relative stabilities were computed in a systematic fashion, of which one particular byproduct comprises the novel dihydroxy-bridged structures $M<(OH)_2>M$, for M = Sc, Ti, V.

Reliability of structural parameters and energetics were substantiated, by comparing to previous benchmark calculations on ScO and ScO_2.[9,10] Further support for the computational consistency was found in two recent studies, one on Sc oxide clusters,[11] and one on Ge oxides, oxyhydroxides, and hydroxides.[3] Also, characteristic bond distances in the calculated systems were related to what has previously been determined by means of crystallography, and general agreement was found. This result emphasizes the qualitative validity in using truncated transition metal oxide clusters for investigating the local chemistry of transition metal oxide solids.

A main objective of this project is to provide a comprehensive context for elucidating aspects of recent experimental evidence for accelerated corrosivity of high-temperature alloys in a humid atmosphere.[2] The protective Cr_2O_3(s) scale was seen to erode, and Cr(VI) was observed to condense on the cold parts of the reaction chamber.

An essential common signature in the series of single-bridged M−O−M species (M = Sc, Ti, V, Cr, and Mn) comprises the slight endothermicity in the final hydrolysis step ($\Delta E \sim 20$ kJ/mol), which suggests condensation of mononuclear oxyhydroxides to be preferred under dry conditions. A competitive final product implies stabilization of the mononuclear species by solvation. It is noted that this understanding provides a possible scenario for the stepwise growth of $(-O-(O_2Cr)-)_n$ by condensation, thus explaining the observed formation of CrO_3(s).

The possibility of further emission of water from the binuclear oxyhydroxide was considered for $HO(O_2Cr)O(O_2Cr)OH$, as well as for the other transition metals included in this study. In all cases, water emission was found to be unfavorable. This implies in particular that any $HO(O_2Cr)O(O_2Cr)OH$ molecule, produced at the oxide surface or formed by condensation of chromic acid molecules in the gas phase, would not dehydrate beyond the single-bridged bichromate compound.

Finally, the present study has employed the chemical similarities in the isoelectronic series $(O_3Mn)-O-(MnO_3)$, $HO(O_2Cr)-O-(CrO_2)OH$, and $(HO)_2(OV)-O-(VO)(OH)_2$ to put the properties of chromium oxyhydroxides in perspective. It is gratifying to note that this analogy holds true in the solid state as well. Thus, Mn_2O_7(s) is a molecular solid formed from $(O_3Mn)-O-(MnO_3)$ molecules, while CrO_3(s) and $NaVO_3$(s) consist of $[-O-(O_2Cr)-O-(CrO_2)-]$ and $[-O-(O_2V)^{-}-O-(VO_2)^{-}-]$ chain polymers, respectively.

Acknowledgment. This work was supported by the Swedish Natural Sciences Research Council. Constructive discussions with L.-G. Johansson are acknowledged.

Supporting Information Available: Tables listing detailed structural parameters, absolute energies, and vibrational frequencies. This material is available free of charge via the Internet at http://pubs.acs.org.

IC991144L

(15) (a) Sc_2O_3: Norrestam, R. *Ark. Kemi.* **1968**, *29*, 343. (b) TiO_2: Baur, W. H. *Acta Crystallogr.* **1961**, *14*, 214. (c) V_2O_5: Bachmann, H. G.; Ahmed, F. R.; Barnes, W. H. *Z. Kristallogr.* **1961**, *115*, 110. (d) CrO_3: Stephens, J. S.; Cruickshank, D. W. J. *Acta Crystallogr.* **1970**, *B26*, 222. (e) Mn_2O_7: Dronkowski, R.; Krebs, B.; Simon, A.; Miller, G.; Hettich, B. *Z. Anorg. Chem.* **1988**, *558*, 7.